

Elliptic flow of electrons from beauty-hadron decays extracted from Pb–Pb collision data at $\sqrt{s_{\text{NN}}} = 2.76$ TeV

D. Moreira de Godoy^{1,a} , F. Herrmann¹, M. Klasen¹, C. Klein-Bösing^{1,2}, A. A. P. Suaide³

¹ Westfälische Wilhelms-Universität Münster, Wilhelm-Klemm-Straße 9, Münster, Germany

² ExtreMe Matter Institute EMMI, GSI Helmholtzzentrum für Schwerionenforschung, Planckstraße 1, 64291 Darmstadt, Germany

³ Universidade de São Paulo, R. do Matão 1371, São Paulo, Brazil

Received: 24 September 2017 / Accepted: 26 April 2018 / Published online: 21 May 2018
© The Author(s) 2018

Abstract We present a calculation of the elliptic flow of electrons from beauty-hadron decays in semi-central Pb–Pb collisions at centre-of-mass energy per colliding nucleon pair, represented as $\sqrt{s_{\text{NN}}}$, of 2.76 TeV. The result is obtained by the subtraction of the charm-quark contribution in the elliptic flow of electrons from heavy-flavour hadron decays in semi-central Pb–Pb collisions at $\sqrt{s_{\text{NN}}} = 2.76$ TeV recently made publicly available by the ALICE collaboration.

1 Introduction

The nuclear matter exposed to conditions of high temperature and energy density is expected to undergo a phase transition to a colour deconfined state of matter [1, 2], the Quark-Gluon Plasma (QGP). The conditions for the phase transition can be achieved in the laboratory with collisions of heavy ions at high energies [1]. The properties of the medium formed in the laboratory can be probed with a unique degree of control by particles from decays of heavy flavours (charm and beauty), since heavy quarks are mainly produced in hard parton scattering processes [3–5] at the initial stage of heavy-ion collisions [6, 7] and participate in the entire evolution of the created system. The partons traversing the medium lose energy via collisional and radiative processes [8–12] in the interaction with the medium constituents. The energy loss of partons is predicted to be dependent on their colour charge and mass, resulting in a hierarchy where beauty quarks lose less energy than charm quarks, charm quarks lose less energy than light quarks, and quarks lose less energy than gluons [10, 13, 14]. The heavy-flavour energy loss can be investigated experimentally with the nuclear modification factor (R_{AA}) of heavy-flavour particles, defined as

$$R_{\text{AA}} = \frac{1}{\langle T_{\text{AA}} \rangle} \frac{dN_{\text{AA}}/dp_{\text{T}}}{d\sigma_{\text{pp}}/dp_{\text{T}}}, \quad (1)$$

where $dN_{\text{AA}}/dp_{\text{T}}$ is the transverse momentum (p_{T}) differential yield in nucleus-nucleus (AA) collisions; $\langle T_{\text{AA}} \rangle$ is the average nuclear overlap function in nucleus-nucleus collisions, given by the ratio of the average number of binary collisions and the inelastic cross section; and $d\sigma_{\text{pp}}/dp_{\text{T}}$ is the p_{T} -differential cross section in proton-proton (pp) collisions. A suppression of the yield of D mesons and leptons from heavy-flavour hadron decays ($R_{\text{AA}} < 1$) for $p_{\text{T}} > 3$ GeV/c was observed in gold–gold (Au–Au) collisions at $\sqrt{s_{\text{NN}}} = 200$ GeV at the Relativistic Heavy Ion Collider (RHIC) [15–18] and in lead–lead (Pb–Pb) collisions at $\sqrt{s_{\text{NN}}} = 2.76$ and 5.02 TeV at the Large Hadron Collider (LHC) [19–25], indicating energy loss of heavy flavours in the medium. An experimental hint to the quark mass dependence of the heavy-flavour energy loss has been found in the comparison of the R_{AA} of D mesons and non-prompt J/ψ from B-hadron decays in central Pb–Pb collisions at $\sqrt{s_{\text{NN}}} = 2.76$ TeV at the LHC [20, 26, 27]. The observed difference of these measurements is described by model calculations [28, 29] as predominantly due to the quark mass dependence of the parton energy loss.

The interaction of heavy quarks with the medium can be further investigated with the azimuthal anisotropy of heavy-flavour particles, extracted from the coefficients v_n of the Fourier decomposition of the particle azimuthal distribution in the transverse plane [30]

$$\frac{dN}{d(\varphi - \Psi_n)} \propto 1 + 2 \sum_{n=1}^{\infty} v_n \cos [n(\varphi - \Psi_n)], \quad (2)$$

where φ is the azimuthal angle of the heavy-flavour particles and Ψ_n is the symmetry-plane angle of the n th-order harmonic. The second Fourier coefficient v_2 , called elliptic

^a e-mail: moreirad@uni-muenster.de

flow, quantifies the elliptic azimuthal anisotropy of the emitted particles. The origin of the elliptic azimuthal anisotropy of heavy-flavour particles in non-central heavy-ion collisions depends on the transverse-momentum interval. While the v_2 at low p_T is sensitive to the collective motion of the medium constituents caused by pressure gradients, the v_2 at high p_T can constrain the path-length dependence of the in-medium energy loss of heavy quarks, resulting from the direction of the particles that traverse the ellipsoidal nuclear overlap region. The elliptic flow of prompt D mesons at mid-rapidity is observed to be positive in 30–50% Pb–Pb collisions at $\sqrt{s_{NN}} = 2.76$ TeV at the LHC [31,32] with 5.7σ significance in the interval $2 < p_T < 6$ GeV/c, indicating that charm quarks participate in the collective motion of the system. Measurements of the prompt D-meson v_2 in Pb–Pb collisions at $\sqrt{s_{NN}} = 5.02$ TeV [33,34] have smaller uncertainties compared to the ones in Pb–Pb collisions at $\sqrt{s_{NN}} = 2.76$ TeV. The results at the two collision energies are compatible within uncertainties. The prompt $D_s^+ v_2$ in semi-central Pb–Pb collisions at $\sqrt{s_{NN}} = 5.02$ TeV is compatible within uncertainties with the average of prompt D^0 , D^+ , and $D^{*+} v_2$ in the same collision system [34]. A positive v_2 is also observed for leptons from heavy-flavour hadron decays at low and intermediate p_T in semi-central Au–Au collisions at $\sqrt{s_{NN}} = 200$ GeV at RHIC [17,35] and in semi-central Pb–Pb collisions at $\sqrt{s_{NN}} = 2.76$ TeV at the LHC [25,36,37]. In particular, the v_2 of electrons from heavy-flavour hadron decays is observed to be positive with 5.9σ significance in the range $2 < p_T < 2.5$ GeV/c in 20–40% Pb–Pb collisions at $\sqrt{s_{NN}} = 2.76$ TeV.

In view of the experimental results on the elliptic flow of heavy-flavour particles, an important question that remains open is whether beauty quarks take part in the collective motion in the medium. The first measurement of the v_2 of non-prompt J/ψ mesons from B-hadron decays is compatible with zero within uncertainties in two kinematic regions, $6.5 < p_T < 30$ GeV/c and $|y| < 2.4$, and $3 < p_T < 6.5$ GeV/c and $1.6 < |y| < 2.4$, in 10–60% Pb–Pb collisions at $\sqrt{s_{NN}} = 2.76$ TeV at the LHC [27]. In this paper, we present a method to subtract the contribution of charm quarks in the published measurement of the elliptic flow of electrons from heavy-flavour hadron decays in semi-central Pb–Pb collisions at $\sqrt{s_{NN}} = 2.76$ TeV performed by the ALICE collaboration. The calculation uses as input the v_2 coefficients of prompt D mesons and electrons from heavy-flavour hadron decays measured by the ALICE collaboration [32,36] and three different results for the relative contribution of electrons from beauty-hadron decays to the yield of electrons from heavy-flavour hadron decays [38–41].

2 Methodology

The particle azimuthal distribution of electrons from heavy-flavour hadron decays ($e \leftarrow c + b$) can be separated into the contributions of electrons from charm-hadron decays ($e \leftarrow c$) and from beauty-hadron decays ($e \leftarrow b$). Consequently, the elliptic flow of electrons from beauty-hadron decays can be expressed as

$$v_2^{e \leftarrow b} = \frac{v_2^{e \leftarrow c+b} - (1 - R)v_2^{e \leftarrow c}}{R}, \quad (3)$$

where R represents the relative contribution of electrons from beauty-hadron decays to the yield of electrons from heavy-flavour hadron decays.

In the following, we present the currently published measurements and, in case there is no available measurement, our calculations of the three observables required to obtain the elliptic flow of electrons from beauty-hadron decays. Based on available results on open heavy flavours at RHIC and LHC, the most suitable system for this analysis is the Pb–Pb collision system at $\sqrt{s_{NN}} = 2.76$ TeV in the 20–40% centrality class, which corresponds to the centrality range where the measured v_2 of electrons from heavy-flavour hadron decays is observed to be positive with a maximum significance [36] and thus a possible elliptic flow of electrons from beauty-hadron decays is expected to be more significant. In this analysis, the v_2 and R_{AA} of heavy-flavour particles are assumed to be the same at slightly different mid-rapidity ranges ($|y| < 0.5$, 0.7 and 0.8) in which the measurements needed in the calculation are available. Indeed, no dependence on rapidity was observed in recent ALICE results on those observables for electrons from heavy-flavour hadron decays at mid-rapidity ($|y| < 0.7$ for v_2 and $|y| < 0.6$ for R_{AA} measurements) and muons from heavy-flavour hadron decays at forward rapidity ($2.5 < y < 4$) [24,36].

2.1 Elliptic flow of electrons from heavy-flavour hadron decays

The result on the elliptic flow of electrons from heavy-flavour hadron decays ($v_2^{e \leftarrow c+b}$) at mid-rapidity ($|y| < 0.7$) in 20–40% Pb–Pb collisions at $\sqrt{s_{NN}} = 2.76$ TeV published by the ALICE collaboration [36] is used in this analysis. The $v_2^{e \leftarrow c+b}$ is measured in the interval $0.5 < p_T < 13$ GeV/c with the event plane method [30]. A positive value is observed in the interval $2 < p_T < 2.5$ GeV/c with significance of 5.9σ [36].

2.2 Relative contribution of electrons from beauty-hadron decays to the yield of electrons from heavy-flavour hadron decays

The measurement of the relative contribution of electrons from beauty-hadron decays to the yield of electrons from heavy-flavour hadron decays (R) has been published by the ALICE collaboration only in pp collisions at $\sqrt{s} = 2.76$ TeV [38,39]. The factor R is measured using the track impact parameter and electron-hadron azimuthal correlation methods. Results obtained with both techniques are compatible within uncertainties. The coefficient R measured in pp collisions with the electron-hadron azimuthal correlation method is used in the analysis with the caveat that initial- and final-state effects modify the yield of electrons from heavy-flavour hadron decays in heavy-ion collisions. In particular, the coefficient R at high p_T is expected to be higher in Pb–Pb collisions compared to pp collisions, since the in-medium energy loss of charm quarks is predicted to be larger than the one of beauty quarks [23]. Therefore, the factor R at high p_T in Pb–Pb collisions at $\sqrt{s_{NN}} = 2.76$ TeV is expected to have an exclusive value between the measured factor R in pp collisions at $\sqrt{s} = 2.76$ TeV and unity. Consequently, according to Eq. 3, the minimum value of the v_2 of electrons from beauty-hadron decays can be computed with the R measured in pp collisions.

In addition to the available measurement, the coefficient R is obtained with a Monte Carlo (MC) simulation based on POWHEG [42], which provides the calculation of the heavy-flavour production in hadronic collisions at Next-to-Leading Order (NLO) accuracy. The POWHEG results are interfaced to PYTHIA [43,44] in order to generate the shower, hadronisation and decay. In agreement with other heavy-flavour production tools, e.g. pQCD calculation at Fixed Order plus Next-to-Leading Logarithms (FONLL) [4,45] and earlier pp calculations [5], the square root of the quadratic sum of the quark mass (m_Q) and p_T are used as renormalization and factorization scales, i.e. $\mu = \mu_f = \mu_r = \sqrt{m_Q^2 + p_T^2}$. The charm- and beauty-quark masses are set as 1.5 and 4.75 GeV, respectively. Even though the calculated coefficient R is sensitive to the choice of heavy-quark masses and scales [5], only the central value is shown in this analysis. Admittedly, the described framework is designed for pp collisions, but by making use of the EPS09 [46] NLO nuclear Parton Distribution Functions (nPDFs) the framework is able to account for initial-state cold nuclear effects. The nPDF gluon shadowing results in reduced p_T -differential cross sections for electrons from heavy-flavour hadron decays for $p_T < 6$ GeV/c and affects contributions from charm quarks stronger than those from beauty quarks. Thus, it provides a lower baseline for the factor R , which is suggested to be further enhanced by medium interactions as it will be discussed in this paper. In

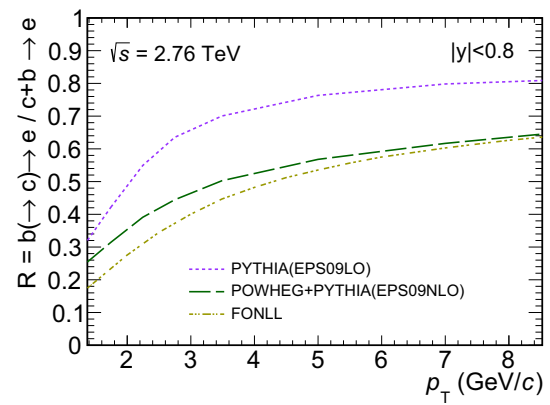


Fig. 1 Comparison of the relative contribution of electrons from beauty-hadron decays to the yield of electrons from heavy-flavour hadron decays (R) at $\sqrt{s} = 2.76$ TeV obtained with POWHEG+PYTHIA [42–44] at NLO accuracy using EPoS09 NLO nPDFs, with PYTHIA at LO accuracy using EPoS09 LO nPDFs, and with FONLL calculation [4,45] using CTEQ6.6 PDFs. Only the central values are shown

addition, the R coefficient is also obtained with a leading order (LO) calculation based on PYTHIA using EPoS09 LO nPDFs to study the impact of NLO corrections [5]. The comparison of the calculations with LO and NLO approaches, shown in Fig. 1, reveals that the factor R is reduced with the NLO corrections, stressing the importance of NLO calculations. In fact, the additional processes of heavy-flavour production at NLO give rise to large logarithmic corrections to the charm- and beauty-quark cross sections depending on the heavy-flavour mass. The corresponding FONLL calculation of the factor R using CTEQ6.6 PDFs, which is also shown in Fig. 1, is similar to the POWHEG+PYTHIA(EPoS09NLO) result at high p_T .

The result on the factor R from the BAMPS heavy-flavour transport model [40,41], which includes collisional and radiative in-medium energy loss of heavy quarks, is also employed in the analysis to obtain the v_2 of electrons from beauty-hadron decays. The choice of the BAMPS model is justified by the good agreement of the predictions for the R_{AA} of electrons from beauty- and heavy-flavour hadron decays for $p_T > 3$ GeV/c in central Pb–Pb collisions at $\sqrt{s_{NN}} = 2.76$ TeV with what measured by the ALICE collaboration [23,24].

In this analysis, the R coefficient measured in pp collisions using the electron-hadron azimuthal correlation technique and the ones obtained with POWHEG + PYTHIA (EPoS09NLO) and with the BAMPS model are used to estimate the elliptic flow of electrons from beauty-hadron decays.

2.3 Elliptic flow of electrons from charm-hadron decays

The elliptic flow of electrons from charm-hadron decays ($v_2^{e \leftarrow c}$) is estimated using a MC simulation of decays of D^0

mesons into electrons with PYTHIA. The MC simulation is based on two observables measured for D^0 mesons in Pb–Pb collisions at $\sqrt{s_{NN}} = 2.76$ TeV:

- the p_T -differential yield, which is used as a probability distribution for finding a D^0 meson with a certain p_T ;
- the p_T -differential v_2 , which is used to obtain the $\varphi_{D^0} - \Psi_2$ probability distribution with Eq. 2.

In fact, the p_T -differential yield of D^0 mesons at mid-rapidity ($|y| < 0.8$) in 20–40% Pb–Pb collisions at $\sqrt{s_{NN}} = 2.76$ TeV is estimated from the ALICE results on the p_T -differential yield and R_{AA} of prompt D^0 mesons at mid-rapidity ($|y| < 0.5$) in 0–20% Pb–Pb collisions at the same collision energy [19] as

$$\left(\frac{dN_{AA}}{dp_T}\right)^{20-40\%} = C_{\Delta y} C_{(T_{AA})} C_{R_{AA}} \left(\frac{dN_{AA}}{dp_T}\right)^{0-20\%}, \quad (4)$$

where the coefficient $C_{\Delta y} = 1.6$ corresponds to the scaling factor of the yield from $|y| < 0.5$ to $|y| < 0.8$ in pp collisions, assuming a uniform distribution of the D^0 -meson yield within the rapidity range. The terms $C_{(T_{AA})} = 0.362 \pm 0.020$ [19] and $C_{R_{AA}}$ are the ratios of the average nuclear overlap function and the D^0 -meson R_{AA} , respectively, in Pb–Pb collisions at $\sqrt{s_{NN}} = 2.76$ TeV in the 20–40% centrality class to the ones in the 0–20% centrality class. Note that the terms $C_{\Delta y}$ and $C_{(T_{AA})}$ are constant, so they do not play a role in the determination of the D^0 -meson p_T probability distribution. The non-measured R_{AA} of D^0 mesons in 20–40% Pb–Pb collisions at $\sqrt{s_{NN}} = 2.76$ TeV is estimated by the average of the ALICE results on the D^0 -meson R_{AA} in Pb–Pb collisions at the same collision energy in the 0–20 and 40–80% centrality classes [19] weighted by the corresponding yield of D^0 mesons in each centrality class. The resulting p_T distribution of D^0 mesons in 20–40% Pb–Pb collisions obtained from Eq. 4 is then fitted by a power-law function (top panel of Fig. 2), considering the statistical uncertainty of the experimental results. The fit function is used as the D^0 -meson p_T probability distribution.

The v_2 of prompt D^0 mesons in 20–40% Pb–Pb collisions at $\sqrt{s_{NN}} = 2.76$ TeV (bottom panel of Fig. 2) is obtained by the arithmetic average of the measured prompt D^0 -meson v_2 in Pb–Pb collisions at the same collision energy in the 10–30 and 30–50% centrality classes [32]. Indeed, experimental results show that the v_2 of heavy-flavour particles increases with the centrality class [17,32,36,37], which is consistent with the qualitative expectation of increasing of the elliptic anisotropy from central to peripheral nucleus-nucleus collisions. The statistical and systematic uncertainties are propagated considering the prompt D^0 -meson v_2 in the 10–30 and

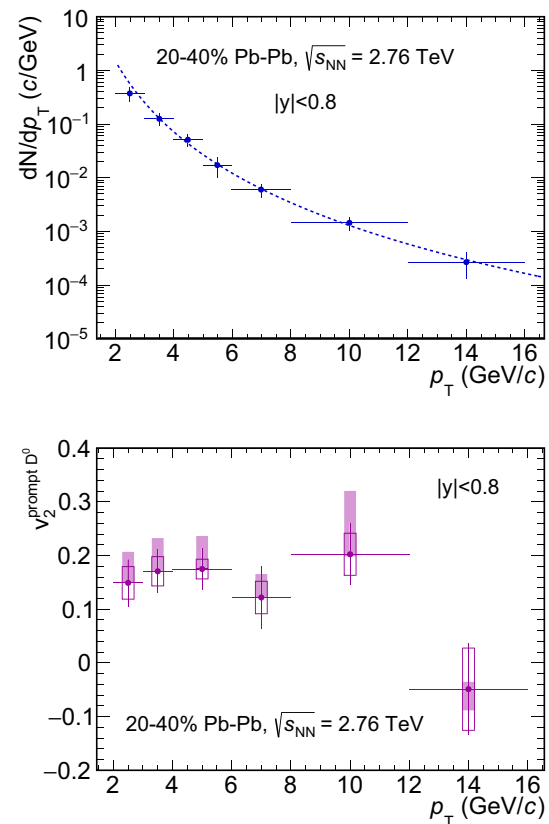


Fig. 2 Top: estimated p_T -differential yield of D^0 mesons in 20–40% Pb–Pb collisions at $\sqrt{s_{NN}} = 2.76$ TeV from ALICE results [19]. The dashed line corresponds to the power-law fitted function. Bottom: estimated v_2 of prompt D^0 mesons in 20–40% Pb–Pb collisions at $\sqrt{s_{NN}} = 2.76$ TeV from ALICE results [32]. The vertical error bars represent the statistical uncertainties and the horizontal error bars indicate the bin widths. The empty and filled boxes represent the systematic uncertainties from data and from the B feed-down subtraction, respectively, in the D^0 -meson v_2 measurement [32]

30–50% centrality classes as uncorrelated as a conservative estimation. In the D^0 -meson v_2 measurement by the ALICE collaboration, the central value was obtained by assuming that the v_2 coefficients of prompt D mesons and D mesons from B-meson decays are the same [32]. However, the systematic uncertainty related to this assumption, referred to as systematic uncertainty from the B feed-down subtraction, was evaluated by the ALICE collaboration. It was assumed that the v_2 of prompt D mesons from B-meson decays should be between zero and v_2 of prompt D mesons, resulting in the upper and lower limits of the systematic uncertainty, respectively. Therefore, the B feed-down contribution decreases the absolute value of the D^0 -meson v_2 and thus the systematic uncertainty is restricted to the upper (lower) limit when the v_2 is positive (negative). Since the measured D^0 -meson v_2 coefficients are negative in the $8 < p_T < 12$ and $12 < p_T < 16$ GeV/c intervals in the 10–30 and 30–50% centrality classes, respectively, the resulting propagated systematic uncertainty

from the B feed-down subtraction contains lower and upper limits.

Finally, the estimated p_T and v_2 distributions of D^0 mesons in 20–40% Pb–Pb collisions at $\sqrt{s_{NN}} = 2.76$ TeV are used to obtain the $v_2^{\leftarrow c} = \langle \cos [2(\varphi_e - \Psi_2)] \rangle$ in the same collision system using the PYTHIA event generator. The azimuthal angle of electrons (φ_e) takes into account the angular separation between electrons and their parent D^0 mesons.

2.3.1 Statistical uncertainty

The statistical uncertainty of the D^0 -meson v_2 is used as input for the MC simulation to obtain the statistical uncertainty of the $v_2^{\leftarrow c}$. The statistical uncertainties of the measurements used to obtain the p_T -differential yield of D^0 mesons are considered in the fit of the D^0 -meson probability distribution. Further variations are considered as systematic uncertainties.

2.3.2 Systematic uncertainty

The systematic uncertainties from data and from the B feed-down subtraction of the D^0 -meson v_2 (bottom panel of Fig. 2) are used as input for the MC simulation to obtain the systematic uncertainty of the $v_2^{\leftarrow c}$. The following is a discussion on other sources of systematic uncertainty that can influence the $v_2^{\leftarrow c}$ estimation.

In order to validate the Eq. 4, the p_T -differential yield and R_{AA} of prompt D^0 mesons in 40–80% Pb–Pb collisions at $\sqrt{s_{NN}} = 2.76$ TeV [19] are also used as reference to obtain the p_T -differential yield of D^0 mesons in the 20–40% centrality class. The result is the same as the one obtained with the 0–20% centrality class (top panel of Fig. 2).

The ALICE result on the D^0 -meson R_{AA} in the 30–50% centrality class [32] is used as an alternative for the D^0 -meson R_{AA} estimation in the 20–40% centrality class. No significant difference is observed in the resulting $v_2^{\leftarrow c}$ with respect to the one obtained with the R_{AA} estimated by the average of the D^0 -meson R_{AA} measurements in the 0–20 and 40–80% centrality classes weighted by the corresponding yield of D^0 mesons in each centrality class.

The systematic uncertainties of the measurements of the p_T -differential yield and R_{AA} of prompt D^0 mesons are considered in the fit of the D^0 -meson p_T distribution in 20–40% Pb–Pb collisions. No significant difference is observed in the resulting $v_2^{\leftarrow c}$ with respect to the one considering only the statistical uncertainty in the fit. For further investigation, The BAMPS result on the p_T distribution of D mesons at $|y| < 0.8$ in 20–40% Pb–Pb collisions at $\sqrt{s_{NN}} = 2.76$ TeV [40, 41] is also used to compute the $v_2^{\leftarrow c}$. The relative difference of the obtained $v_2^{\leftarrow c}$ using the estimated p_T distribution of D^0 mesons and the BAMPS result, which increases from 1 to

20% in the interval $2 < p_T < 8$ GeV/c, is included in the systematic uncertainty.

The effect of the D^0 -meson v_2 estimation in 20–40% Pb–Pb collisions using the arithmetic average of the D^0 -meson v_2 measurements in the 10–30 and 30–50% centrality classes is investigated in this analysis. For this purpose, the trend of the unidentified charged particle v_2 as a function of the average number of binary collisions ($\langle N_{coll} \rangle$) [47] is assumed to be the same as the one for D^0 mesons. The v_2 as a function of $\langle N_{coll} \rangle$ is obtained from a parametrisation of the centrality-dependent v_2 measurement of unidentified charged particles integrated over the interval $0.2 < p_T < 5$ GeV/c [48]. The corresponding result exhibits a linear dependence between v_2 and $\langle N_{coll} \rangle$ with a negative slope for $\langle N_{coll} \rangle > 220$. For comparison, the parametrisation is also obtained from the centrality-dependent v_2 measurement of unidentified charged particles integrated over the interval $10 < p_T < 20$ GeV/c [49]. The linear dependence between v_2 and $\langle N_{coll} \rangle$ is the same as the one obtained for particles in a lower p_T interval. The D^0 -meson v_2 is then obtained by the average of the D^0 -meson v_2 in the 10–30 and 30–50% centrality classes weighted by the v_2 coefficients of the corresponding $\langle N_{coll} \rangle$ values [47]. The relative difference of the obtained D^0 -meson v_2 with respect to the one obtained with the arithmetic average is negligible for $p_T < 8$ GeV/c and its average is 19% for $p_T > 8$ GeV/c, which is still compatible within uncertainties. The $v_2^{\leftarrow c}$ coefficients obtained with the two approaches show a relative difference of 2% in the range $2 < p_T < 8$ GeV/c. This deviation is considered as a consequence of statistical fluctuations in the D^0 -meson v_2 measurement for $p_T > 8$ GeV/c and thus no systematic uncertainty is assigned for this effect.

In order to investigate the impact of the assumption of the particle mass ordering of the elliptic flow [50] used to determine the systematic uncertainty from the B feed-down subtraction in the D^0 -meson v_2 measurement, one can assume that the v_2 of prompt D mesons from B-meson decays should be between zero and the unidentified charged particle v_2 . The unidentified charged particle v_2 in 20–40% Pb–Pb collisions is obtained by the average of the v_2 measurements in the 20–30 and 30–40% centrality classes [49] weighted by the corresponding $\langle N_{coll} \rangle$ values. The v_2 coefficients of prompt D^0 mesons and unidentified charged particles are compatible within uncertainties as well as the $v_2^{\leftarrow c}$ obtained with these two results. Therefore, the lower limit of the systematic uncertainty from the B feed-down subtraction can be positioned at the central values of the prompt D-meson v_2 and $v_2^{\leftarrow c}$ without strictly considering that the B-meson v_2 is expected to be lower than the D-meson v_2 .

As a consequence of the p_T interval ($2 < p_T < 16$ GeV/c) of the D^0 -meson v_2 and p_T -differential yield measurements, the $v_2^{\leftarrow c}$ is obtained in the range $2 < p_T < 8$ GeV/c. The fraction of electrons with $p_T > 2$ GeV/c

that come from D^0 mesons with $p_T < 2$ GeV/c is negligible according to PYTHIA simulations. The effect of the p_T upper limit of the D^0 -meson measurements is studied by evaluating the $v_2^{e\leftarrow c}$ with extrapolation of the p_T and v_2 distributions of D^0 mesons up to 26 GeV/c. The transverse momentum extrapolation is obtained from the power-law fit function shown in the top panel of Fig. 2, while the impact of the v_2 of D^0 mesons is estimated by explicitly setting its value, in the interval $16 < p_T < 26$ GeV/c, to either zero, or constant at high p_T , or maximum value of the prompt D^0 -meson v_2 (shown in Fig. 2). The highest relative difference in these three scenarios, which increases from 0.3 to 40% in the interval $2 < p_T < 8$ GeV/c, is assigned as a conservative systematic uncertainty.

The effect of the mid-rapidity range of D^0 mesons is investigated by obtaining the $v_2^{e\leftarrow c}$ using the D^0 -meson p_T distribution in the rapidity range $|y| < 1.6$ as input for the simulation. The D^0 -meson v_2 is considered to be the same in this rapidity range, because no dependence on rapidity was observed in ALICE results on leptons from heavy-flavour hadron decays [24, 36] as discussed previously. The relative difference of the obtained $v_2^{e\leftarrow c}$ with respect to the one using the D^0 -meson p_T distribution in the rapidity range $|y| < 0.8$ is negligible and thus no additional systematic uncertainty is considered due to the rapidity effect.

In this analysis, the v_2 and shape of the p_T -differential yields of charm hadrons are assumed to be the same as the ones measured for D^0 mesons. This is justified by the fact that the v_2 coefficients of D^0 , D^+ and D^{*+} mesons are compatible within uncertainties in 30–50% Pb–Pb collisions at $\sqrt{s_{NN}} = 2.76$ TeV [31], also the prompt $D_s^+ v_2$ is compatible within uncertainties with the prompt non-strange D meson v_2 in 30–50% Pb–Pb collisions at $\sqrt{s_{NN}} = 5.02$ TeV [34]. In addition, the ratios of the yields of D^+/D^0 and D^{*+}/D^0 were observed to be constant within uncertainties in pp collisions at $\sqrt{s} = 7$ TeV and no modification of the ratios was observed within uncertainties in central and semi-central Pb–Pb collisions at $\sqrt{s_{NN}} = 2.76$ TeV [51]. A possible hint for an enhancement of the D_s^+/D^0 ratio is observed in 0–10% Pb–Pb collisions at $\sqrt{s_{NN}} = 2.76$ TeV [52], but the current uncertainties do not allow for a conclusion. The effect of different decay kinematics of charm particles is estimated by simulating the v_2 of electrons from combined D, D^* , D_s , and Λ_c particle decays taking into account the fraction of charm quarks that hadronise into these particles [53] and using the same simulation input as used in the analysis (p_T -differential yield and v_2 of D^0 mesons). The obtained $v_2^{e\leftarrow c}$ is compatible with the one using D^0 -meson decay and thus no systematic uncertainty is considered due to this effect. In order to exemplify the impact of a possible production enhancement of D_s^+ and Λ_c particles in Pb–Pb collisions with respect to pp collisions, their fragmentation fractions are increased by a factor 2 and 5, respectively, in the sim-

ulation of the combined charm meson v_2 . The relative difference of the obtained $v_2^{e\leftarrow c}$ and the one using D^0 -meson decay is negligible for $p_T < 3$ GeV/c and its average is 5% for $p_T > 3$ GeV/c.

Finally, the D^0 -meson v_2 systematic uncertainty from data is summed in quadrature with other sources of systematic uncertainty that affect significantly the $v_2^{e\leftarrow c}$ estimation, which are the p_T distribution of D^0 mesons and the limited p_T interval of the D^0 -meson measurements. They are considered as uncorrelated since the effect from the p_T distribution of D^0 mesons is obtained with the BAMPS result and the effect from the limited p_T interval of the D^0 -meson measurements is obtained by extrapolations. The term “from data” is maintained later in this paper to distinguish all sources of systematic uncertainty from the systematic uncertainty related to the B feed-down subtraction of the D^0 -meson v_2 measurement, which is shown separately.

2.4 Elliptic flow of electrons from beauty-hadron decays

The v_2 of electrons from beauty-hadron decays ($v_2^{e\leftarrow b}$) is obtained from Eq. 3 using the R , $v_2^{e\leftarrow c+b}$ and $v_2^{e\leftarrow c}$ results presented in their respective sections.

The three results are considered as statistically independent. First, the factor R was measured in a different collision system (pp collisions) or obtained with calculations. Second, the $v_2^{e\leftarrow c}$ is obtained with a simulation using measurements of D^0 mesons reconstructed via the hadronic decay channel $D^0 \rightarrow K^- \pi^+$ in a different centrality class than in the $v_2^{e\leftarrow c+b}$ measurement.

Even though the systematic uncertainties of the R , $v_2^{e\leftarrow c+b}$ and $v_2^{e\leftarrow c}$ results might be partially correlated, especially concerning the particle identification selection criteria, the limited public information prevents a more accurate treatment of these uncertainties. Therefore, they are assumed to be uncorrelated as a conservative estimation. As an example of the effect of a possible overestimation, if the systematic uncertainties of the $v_2^{e\leftarrow c}$ and $v_2^{e\leftarrow c+b}$ results decrease by 30% in the interval $2 < p_T < 8$ GeV/c, the systematic uncertainty from data of the $v_2^{e\leftarrow b}$ result is expected to decrease by approximately 24%.

Therefore, the statistical and systematic uncertainties of the R , $v_2^{e\leftarrow c+b}$ and $v_2^{e\leftarrow c}$ results are propagated as independent variables. The $v_2^{e\leftarrow b}$ systematic uncertainties from data and from the B feed-down subtraction are asymmetric as a consequence of the systematic uncertainty asymmetry of the measurements used in this analysis. The systematic uncertainty from data is evaluated according to the method described in [54], where the positive and negative deviations are obtained separately and their average is added in quadrature. For verification, the alternative approach presented in [55] is also applied in this analysis. No signifi-

cant difference between these methods is observed. Since the asymmetry of the systematic uncertainty from the B feed-down subtraction only comes from the $v_2^{\ell \leftarrow c}$ result, the limits of the $v_2^{\ell \leftarrow b}$ systematic uncertainty are the deviations resulting from the upper and lower limits of the $v_2^{\ell \leftarrow c}$ systematic uncertainty.

3 Results

The relative contribution of electrons from beauty-hadron decays to the yield of electrons from heavy-flavour hadron decays at $\sqrt{s} = 2.76$ TeV obtained with POWHEG + PYTHIA at NLO accuracy using EPS09 NLO nPDFs is shown in the top panel of Fig. 3. The result is compared with the R in pp collisions at $\sqrt{s} = 2.76$ TeV measured by the ALICE collaboration using the electron-hadron azimuthal correlation technique [38,39] and with the BAMPS result in 20–40% Pb–Pb collisions at $\sqrt{s_{NN}} = 2.76$ TeV [40]. The comparison shows that R is higher when in-medium effects are present, which is consistent with the expectation of the mass hierarchy of the energy loss of charm and beauty quarks in the medium. The bottom panel of Fig. 3 shows the v_2 of electrons from charm-hadron decays at mid-rapidity in 20–40% Pb–Pb collisions at $\sqrt{s_{NN}} = 2.76$ TeV obtained with a MC simulation with PYTHIA using as input the p_T -differential yield and v_2 distributions of D^0 mesons in the same collision system. A positive v_2 of electrons from charm-hadron decays is found in all p_T intervals, with a maximum significance of $3.2\sigma_-$, where σ_- is the combined statistical and systematic uncertainties of the lower limit, in the interval $2 < p_T < 3$ GeV/c.

The v_2 coefficients of electrons from beauty-hadron decays in 20–40% Pb–Pb collisions at $\sqrt{s_{NN}} = 2.76$ TeV obtained with different approaches of the factor R (top panel of Fig. 3) are shown in Fig. 4. The result computed with the coefficient R in pp collisions is an estimation of the minimum value, as discussed previously. The v_2 of electrons from beauty-hadron decays in 20–40% Pb–Pb collisions at $\sqrt{s_{NN}} = 2.76$ TeV is compatible with zero within approximately 1σ of the total uncertainty, obtained by summing in quadrature the different uncertainty contributions, in all p_T intervals and different R coefficients. However, the large statistical and systematic uncertainties prevent a definite conclusion. The result is consistent with the measured v_2 of non-prompt J/ψ mesons from B-hadron decays in 10–60% Pb–Pb collisions at $\sqrt{s_{NN}} = 2.76$ TeV [27], which is also compatible with zero within uncertainties.

Figure 5 shows the v_2 of electrons from charm- and beauty-hadron decays, inclusive [36] and separated, in 20–40% Pb–Pb collisions at $\sqrt{s_{NN}} = 2.76$ TeV. The v_2 of electrons from beauty-hadron decays is lower than the v_2 of electrons from charm-hadron decays, although they are

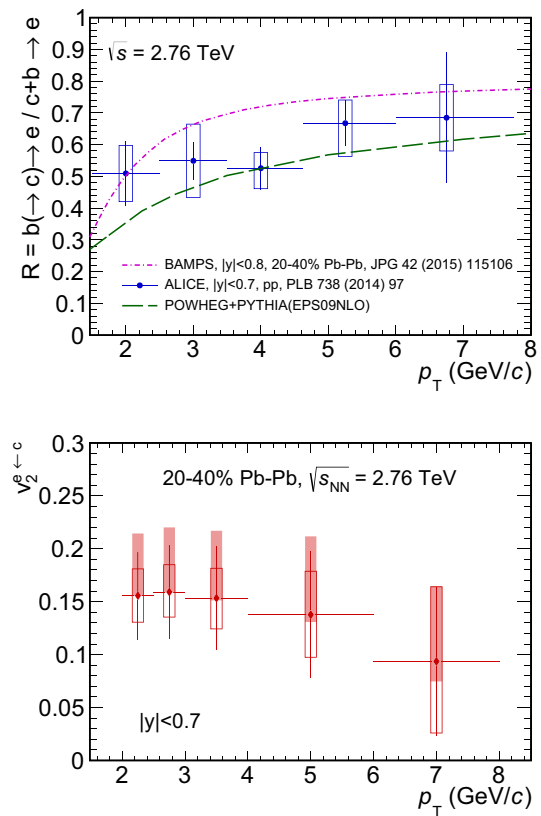


Fig. 3 Top: relative contribution of electrons from beauty-hadron decays to the yield of electrons from heavy-flavour hadron decays at $\sqrt{s} = 2.76$ TeV obtained with POWHEG+PYTHIA at NLO accuracy using EPS09 NLO nPDFs. The result is compared with the R in pp collisions at $\sqrt{s} = 2.76$ TeV measured by the ALICE collaboration using the electron-hadron azimuthal correlation technique [38,39] and with the BAMPS result in 20–40% Pb–Pb collisions at $\sqrt{s_{NN}} = 2.76$ TeV [40]. The statistical and systematic uncertainties of the R coefficient obtained with POWHEG + PYTHIA and from the BAMPS model are zero. Bottom: elliptic flow of electrons from charm-hadron decays at mid-rapidity in 20–40% Pb–Pb collisions at $\sqrt{s_{NN}} = 2.76$ TeV estimated using a MC simulation with PYTHIA based on ALICE results [19,32]. The vertical error bars represent the statistical uncertainties and the horizontal error bars indicate the bin widths. The empty and filled boxes represent the systematic uncertainties from data and from the B feed-down subtraction, respectively, in the D^0 -meson v_2 measurement [32]

compatible within uncertainties. The average of the v_2 coefficients of electrons from charm- and beauty-hadron decays obtained in the interval $2 < p_T < 8$ GeV/c are listed in Table 1. Because of the asymmetric uncertainties, the average is obtained numerically with an iterative sum of the likelihood functions parametrised by variable-width Gaussians [55,56]. The standard deviation, which is the combination of statistical and systematic uncertainties, is assumed to vary linearly. The maximum value of the summed likelihood function corresponds to the average v_2 , while the points at which the function is -0.5 correspond to the lower and upper limits of the total uncertainty.

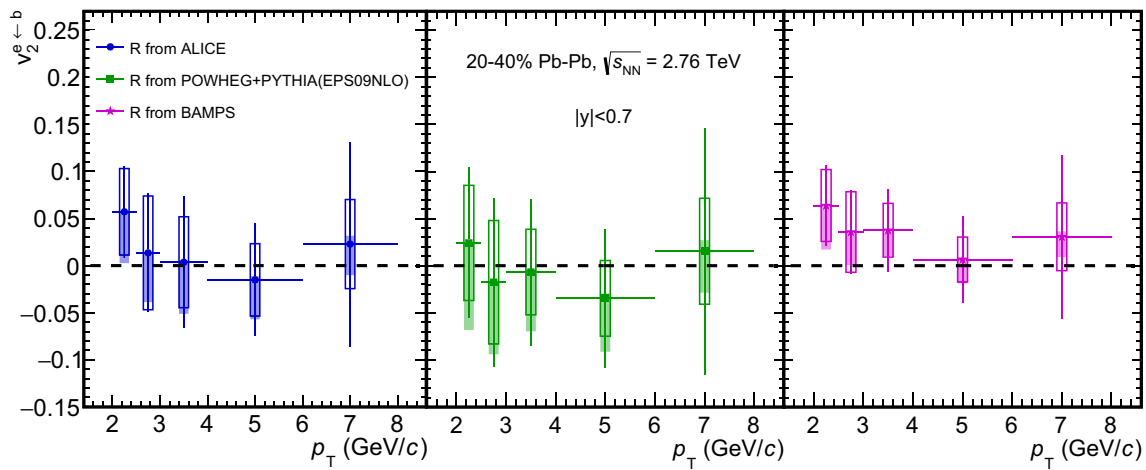


Fig. 4 Elliptic flow of electrons from beauty-hadron decays at mid-rapidity in 20–40% Pb–Pb collisions at $\sqrt{s_{NN}} = 2.76$ TeV using the approaches of the factor R [38–40] shown in the top panel of Fig. 3. The vertical error bars represent the statistical uncertainties and the hor-

izontal error bars indicate the bin widths. The empty and filled boxes represent the systematic uncertainties from data and from the B feed-down subtraction, respectively, in the D^0 -meson v_2 measurement [32]

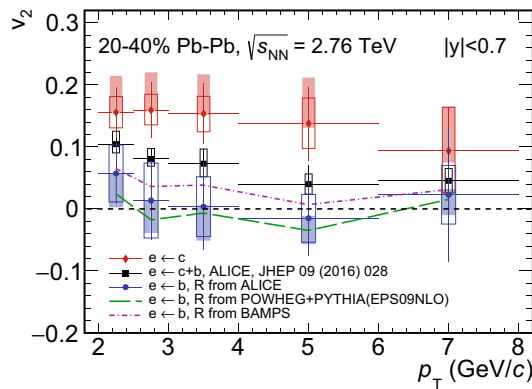


Fig. 5 Elliptic flow of electrons from charm- and beauty-hadron decays, inclusive [36] and separated, in 20–40% Pb–Pb collisions at $\sqrt{s_{NN}} = 2.76$ TeV. The vertical error bars represent the statistical uncertainties and the horizontal error bars indicate the bin widths. The empty and filled boxes represent the systematic uncertainties from data and from the B feed-down subtraction, respectively, in the D^0 -meson v_2 measurement [32]

4 Conclusions

We presented a method to subtract the contribution of charm quarks in the elliptic flow of electrons from heavy-flavour hadron decays. The v_2 of electrons from charm-hadron decays was estimated using a MC simulation of D^0 -meson decays into electrons with PYTHIA, based on measurements of the p_T -differential yield and v_2 of D^0 mesons in Pb–Pb collisions at $\sqrt{s_{NN}} = 2.76$ TeV by ALICE. A positive v_2 of electrons from charm-hadron decays is found with a maximum significance of $3.2\sigma_-$ in the interval $2 < p_T < 3$ GeV/c. The computed v_2 of electrons from charm-hadron decays was then subtracted from the v_2 of electrons from

Table 1 Average of the v_2 coefficients of electrons from charm- and beauty-hadron decays obtained in the transverse momentum interval $2 < p_T < 8$ GeV/c in 20–40% Pb–Pb collisions at $\sqrt{s_{NN}} = 2.76$ TeV. The reported errors are the combined statistical and systematic uncertainties. See text for more details

Result	R approach	Average v_2
$e \leftarrow c$	–	$0.150^{+0.034}_{-0.028}$
$e \leftarrow b$	ALICE	$0.014^{+0.039}_{-0.042}$
$e \leftarrow b$	POWHEG+PYTHIA(EPoS9NLO)	$-0.010^{+0.047}_{-0.052}$
$e \leftarrow b$	BAMPS	$0.032^{+0.028}_{-0.030}$

heavy-flavour hadron decays in 20–40% Pb–Pb collisions at $\sqrt{s_{NN}} = 2.76$ TeV measured by the ALICE collaboration. The subtraction was weighted by the relative contribution of electrons from beauty-hadron decays to the yield of electrons from heavy-flavour hadron decays. Since this observable is not measured in Pb–Pb collisions, three different approaches were used as estimations in the analysis. The resulting v_2 of electrons from beauty-hadron decays in 20–40% Pb–Pb collisions at $\sqrt{s_{NN}} = 2.76$ TeV from the subtraction is compatible with zero within approximately 1σ of the total uncertainty in all p_T intervals and different approaches of the relative contribution of electrons from beauty-hadron decays to the yield of electrons from heavy-flavour hadron decays. However, the large statistical and systematic uncertainties prevent a definite conclusion. The v_2 of electrons from beauty-hadron decays is found to be lower than the v_2 of electrons from charm-hadron decays.

5 Outlook

In the presented method, the elliptic flow of electrons from beauty-hadron decays can be determined by using three

observables that have largely been measured at the LHC and RHIC. Based on available results of these observables, the procedure was applied using measurements performed by the ALICE collaboration. The method demonstrated to be effective; however, the current statistical and systematic uncertainties of the ALICE results prevent a definite conclusion whether the collective motion of the medium constituents influences beauty quarks. A better accuracy of the results on heavy-flavour particles has been achieved in measurements in Pb–Pb collisions at $\sqrt{s_{NN}} = 5.02$ TeV [34] and it is expected to be further improved with the ALICE upgrade, which is foreseen to start in 2019.

In particular, the upgrade of the Inner Tracking System (ITS) detector will improve the determination of the distance of closest approach to the primary vertex, momentum resolution and readout rate capabilities [57]. These improvements will allow for more precise measurements of D mesons down to low transverse momenta and for reducing the systematic uncertainties from data and from the B feed-down subtraction. The latter will be possible with the direct measurement of the fraction of prompt D mesons and D mesons from B-meson decays, which is expected to be accessible with relative statistical and systematic uncertainties smaller than 1 and 5% [57], respectively, for prompt D^0 mesons. In addition, the ITS upgrade will enable the tracking of electrons down to approximately 0.05 GeV/c and enhance the capability to separate prompt from displaced electrons [57], improving the reconstruction of electrons that do not originate from heavy-flavour hadron decays needed for the background subtraction. Moreover, the systematic uncertainty of the elliptic flow of electrons from beauty-hadron decays can be further improved by taking into account correlations among different contributions.

The capability of the heavy-flavour measurements will also enhance with the increase of luminosity. For instance, the current relative statistical uncertainty of the D-meson v_2 measurement in Pb–Pb collisions is 10% for an integrated luminosity of 0.1 nb^{-1} , while it is expected to be 0.2% for a scenario with an integrated luminosity of 10 nb^{-1} [57]. Also the elliptic flow coefficients of D_s and Λ_c particles are expected to be achievable with a relative statistical uncertainty of 8 and 20% [57], respectively.

Therefore, the presented method can be used to extract the elliptic flow of electrons from beauty-hadron decays with better precision with future measurements of the three needed observables.

Acknowledgements We would like to thank Carsten Greiner and Florian Senzel for providing the BAMPS results, as well as Francesco Prino for fruitful discussions. We are grateful for the support of the Deutsche Forschungsgemeinschaft (DFG) through the Research Training Group “GRK 2149: Strong and Weak Interactions—from Hadrons to Dark Matter”; Bundesministerium für Bildung und Forschung (BMBF) under the project number 05P15PMCA1; Conselho Nacional de Desenvolvi-

mento Científico e Tecnológico (CNPq); and Fundação de Amparo à Pesquisa do Estado de São Paulo (FAPESP).

Open Access This article is distributed under the terms of the Creative Commons Attribution 4.0 International License (<http://creativecommons.org/licenses/by/4.0/>), which permits unrestricted use, distribution, and reproduction in any medium, provided you give appropriate credit to the original author(s) and the source, provide a link to the Creative Commons license, and indicate if changes were made. Funded by SCOAP³.

References

1. K. Frithjof, *Lattice QCD at High Temperature and Density* (Springer, Berlin, 2002), pp. 209–249. https://doi.org/10.1007/3-540-45792-5_6
2. P. Petreczky, PoS **ConfinementX**, 028 (2012). <https://pos.sissa.it/171/028/pdf>
3. E. Norrbin, T. Sjostrand, Eur. Phys. J. C **17**, 137 (2000). <https://doi.org/10.1007/s100520000460>
4. M. Cacciari, S. Frixione, N. Houdeau, M.L. Mangano, P. Nason, G. Ridolfi, J. High Energy Phys. **10**, 137 (2012). [https://doi.org/10.1007/JHEP10\(2012\)137](https://doi.org/10.1007/JHEP10(2012)137)
5. M. Klasen, C. Klein-Bösing, K. Kovarik, G. Kramer, M. Topp et al., J. High Energy Phys. **1408**, 109 (2014). [https://doi.org/10.1007/JHEP08\(2014\)109](https://doi.org/10.1007/JHEP08(2014)109)
6. B.W. Zhang, C.M. Ko, W. Liu, Phys. Rev. C **77**, 024901 (2008). <https://doi.org/10.1103/PhysRevC.77.024901>
7. P. Braun-Munzinger, J. Phys. G **34**(8), S471 (2007). <http://stacks.iop.org/0954-3899/34/i=8/a=S36>
8. E. Braaten, M.H. Thoma, Phys. Rev. D **44**, R2625 (1991). <https://doi.org/10.1103/PhysRevD.44.R2625>
9. M. Djordjevic, Phys. Rev. C **74**, 064907 (2006). <https://doi.org/10.1103/PhysRevC.74.064907>
10. S. Wicks, W. Horowitz, M. Djordjevic, M. Gyulassy, Nucl. Phys. A **783**, 493 (2007). <https://doi.org/10.1016/j.nuclphysa.2006.11.102>
11. R. Baier, Y.L. Dokshitzer, A.H. Mueller, S. Peigne, D. Schiff, Nucl. Phys. B **483**, 291 (1997). [https://doi.org/10.1016/S0550-3213\(96\)00553-6](https://doi.org/10.1016/S0550-3213(96)00553-6)
12. M. Djordjevic, U. Heinz, Phys. Rev. C **77**, 024905 (2008). <https://doi.org/10.1103/PhysRevC.77.024905>
13. Y.L. Dokshitzer, D. Kharzeev, Phys. Lett. B **519**, 199 (2001). [https://doi.org/10.1016/S0370-2693\(01\)01130-3](https://doi.org/10.1016/S0370-2693(01)01130-3)
14. N. Armesto, C.A. Salgado, U.A. Wiedemann, Phys. Rev. D **69**, 114003 (2004). <https://doi.org/10.1103/PhysRevD.69.114003>
15. B.I. Abelev et al., Phys. Rev. Lett. **98**, 192301 (2007). <https://doi.org/10.1103/PhysRevLett.98.192301>
16. L. Adamczyk et al., Phys. Rev. Lett. **113**, 142301 (2014). <https://doi.org/10.1103/PhysRevLett.113.142301>
17. A. Adare et al., Phys. Rev. C **84**, 044905 (2011). <https://doi.org/10.1103/PhysRevC.84.044905>
18. S.S. Adler et al., Phys. Rev. Lett. **96**, 032301 (2006). <https://doi.org/10.1103/PhysRevLett.96.032301>
19. B. Abelev et al., J. High Energy Phys. **09**, 112 (2012). [https://doi.org/10.1007/JHEP09\(2012\)112](https://doi.org/10.1007/JHEP09(2012)112)
20. J. Adam et al., J. High Energy Phys. **11**, 205 (2015). [https://doi.org/10.1007/JHEP11\(2015\)205](https://doi.org/10.1007/JHEP11(2015)205). [Addendum: JHEP **06**, 032 (2017)]
21. B. Abelev et al., Phys. Rev. Lett. **109**, 112301 (2012). <https://doi.org/10.1103/PhysRevLett.109.112301>
22. A.M. Sirunyan, et al., CMS-HIN-16-001, CERN-EP-2017-186 (2017). [arXiv:1708.04962](https://arxiv.org/abs/1708.04962)
23. J. Adam et al., J. High Energy Phys. **2017**(7), 52 (2017). [https://doi.org/10.1007/JHEP07\(2017\)052](https://doi.org/10.1007/JHEP07(2017)052)

24. J. Adam et al., Phys. Lett. B **771**, 467 (2017). <https://doi.org/10.1016/j.physletb.2017.05.060>
25. ATLAS, Tech. Rep. ATLAS-CONF-2015-053, CERN (2015). <https://cds.cern.ch/record/2055674>
26. S. Chatrchyan et al., J. High Energy Phys. **05**, 063 (2012). [https://doi.org/10.1007/JHEP05\(2012\)063](https://doi.org/10.1007/JHEP05(2012)063). (CMS-HIN-10-006, CERN-PH-EP-2011-170)
27. V. Khachatryan et al., Eur. Phys. J. C **77**(4), 252 (2017). <https://doi.org/10.1140/epjc/s10052-017-4781-1>
28. M. Djordjevic, M. Djordjevic, B. Blagojevic, Phys. Lett. B **737**, 298 (2014). <https://doi.org/10.1016/j.physletb.2014.08.063>
29. A. Andronic et al., Eur. Phys. J. C **76**(3), 107 (2016). <https://doi.org/10.1140/epjc/s10052-015-3819-5>
30. A.M. Poskanzer, S.A. Voloshin, Phys. Rev. C **58**, 1671 (1998). <https://doi.org/10.1103/PhysRevC.58.1671>
31. B. Abelev et al., Phys. Rev. Lett. **111**, 102301 (2013). <https://doi.org/10.1103/PhysRevLett.111.102301>
32. B.B. Abelev et al., Phys. Rev. C **90**(3), 034904 (2014). <https://doi.org/10.1103/PhysRevC.90.034904>
33. A.M. Sirunyan, et al., CMS-HIN-16-007, CERN-EP-2017-174 (2017). [arXiv:1708.03497](https://arxiv.org/abs/1708.03497)
34. S. Acharya et al., Phys. Rev. Lett. **120**, 102301 (2018). <https://doi.org/10.1103/PhysRevLett.120.102301>
35. L. Adamczyk et al., Phys. Rev. C **95**, 034907 (2017). <https://doi.org/10.1103/PhysRevC.95.034907>
36. J. Adam et al., J. High Energy Phys. **2016**(9), 28 (2016). [https://doi.org/10.1007/JHEP09\(2016\)028](https://doi.org/10.1007/JHEP09(2016)028)
37. J. Adam et al., Phys. Lett. B **753**, 41 (2016). <https://doi.org/10.1016/j.physletb.2015.11.059>
38. B.B. Abelev et al., Phys. Lett. B **738**, 97 (2014). <https://doi.org/10.1016/j.physletb.2014.09.026>
39. B. Abelev et al., Phys. Lett. B **763**, 507 (2016). <https://doi.org/10.1016/j.physletb.2016.10.004>
40. J. Uphoff, O. Fochler, Z. Xu, C. Greiner, J. Phys. G **42**(11), 115106 (2015). <https://doi.org/10.1088/0954-3899/42/11/115106>. <http://stacks.iop.org/0954-3899/42/i=11/a=115106>
41. J. Uphoff, O. Fochler, Z. Xu, C. Greiner, Phys. Lett. B **717**, 430 (2012). <https://doi.org/10.1016/j.physletb.2012.09.069>
42. S. Frixione, P. Nason, G. Ridolfi, J. High Energy Phys. **09**, 126 (2007). <https://doi.org/10.1088/1126-6708/2007/09/126>
43. T. Sjostrand, S. Mrenna, P.Z. Skands, J. High Energy Phys. **05**, 026 (2006). <https://doi.org/10.1088/1126-6708/2006/05/026>. <http://stacks.iop.org/1126-6708/2006/i=05/a=026>
44. T. Sjostrand, S. Mrenna, P.Z. Skands, Comput. Phys. Commun. **178**, 852 (2008). <https://doi.org/10.1016/j.cpc.2008.01.036>
45. M. Cacciari, M. Greco, P. Nason, J. High Energy Phys. **1998**(05), 007 (1998). <http://stacks.iop.org/1126-6708/1998/i=05/a=007>
46. K. Eskola, H. Paukkunen, C. Salgado, J. High Energy Phys. **2009**(04), 065 (2009). <http://stacks.iop.org/1126-6708/2009/i=04/a=065>
47. B. Abelev et al., Phys. Rev. C **88**, 0044909 (2013). <https://doi.org/10.1103/PhysRevC.88.044909>
48. K. Aamodt et al., Phys. Rev. Lett. **105**, 252302 (2010). <https://doi.org/10.1103/PhysRevLett.105.252302>
49. B. Abelev et al., Phys. Lett. B **719**, 18 (2013). <https://doi.org/10.1016/j.physletb.2012.12.066>
50. P.F. Kolb, U.W. Heinz, [arXiv:nucl-th/0305084](https://arxiv.org/abs/nucl-th/0305084) (2003)
51. J. Adam et al., J. High Energy Phys. **2016**(3), 81 (2016). [https://doi.org/10.1007/JHEP03\(2016\)081](https://doi.org/10.1007/JHEP03(2016)081)
52. J. Adam et al., J. High Energy Phys. **2016**(3), 82 (2016). [https://doi.org/10.1007/JHEP03\(2016\)082](https://doi.org/10.1007/JHEP03(2016)082)
53. C. Amsler et al., Review of Particle Physics. Phys. Lett. B **667**(1), 1 (2008). <https://doi.org/10.1016/j.physletb.2008.07.018>. <http://www.sciencedirect.com/science/article/pii/S0370269308008435>
54. G. D'Agostini, (2004). [arXiv:physics/0403086](https://arxiv.org/abs/physics/0403086)
55. R. Barlow, (2003). [arXiv:physics/0306138](https://arxiv.org/abs/physics/0306138)
56. R. Barlow, (2004). [arXiv:physics/0406120](https://arxiv.org/abs/physics/0406120)
57. B. Abelev et al., J. Phys. G **41**(8), 087002 (2014). <https://doi.org/10.1088/0954-3899/41/8/087002>. <http://stacks.iop.org/0954-3899/41/i=8/a=087002>